Supporting Information

Polymer with 3D conductive network: thickness-insensitive electron transport material for inverted polymer solar cells

Zhiquan Zhang, ǂ [ab] Zheling Zhang, ǂ [b] Bin Zhao,[*ac] Youhuan Huang,[b] Jian Xiong,[b] Ping Cai,[b] Xiaogang Xue,[b] Jian Zhang[*b] and Songting Tan[c]

a. Key Laboratory for Green Organic Synthesis and Application of Hunan Province, Key Laboratory of Environmentally Friendly Chemistry and Application of Ministry of Education, College of Chemistry, Xiangtan University, Xiangtan 411105, PR China. Email: xtuzb@163.com

b. College of Material Science & Engineering, Guangxi Key Laboratory of Information Materials, Guilin University of Electrical Technology, Guilin 541004, PR China. Email: jianzhang@guet.edu.cn

c. Key Laboratory of Polymeric Materials & Application Technology of Hunan Province, Xiangtan University, Xiangtan, 411105, PR China.

S1. Experimental section

Preparation of materials: PTB7-Th (1-Material) and $PC_{71}BM$ (Solarmer Materials Inc.) were used as received. PEIE (M_w = 70000 g mol^{-1}, 35-40 wt% in H_2O) and 1,8-diiodooctane (stabilized with copper chip) were acquired from Sigma Aldrich. The PEIE solution was diluted with 2-methoxyethanol to different weight concentration (0.4 wt% for 10 nm, 2.4% for 47 nm). The PEIE-DIO (PEIE-IB) precursor solution, containing PEIE with different weight concentration (0.2 wt% for 9 nm, 1.2 wt% for 50 nm) and DIO (IB) with corresponding weight ratio in 2-methoxyethanol, was prepared by stirring at 70℃ for 8h before spin-coating.

Fabrication of PSCs: The inverted PSC device configuration was ITO/ETLs/PTB7-Th:$PC_{71}BM$ (100 nm)/MoO_3/Ag. The ITO glass substrates were cleaned by sequential ultrasonication in acetone, detergent, deionized water and isopropyl alcohol and then dried with a flowing nitrogen stream. ETLs were prepared by spin coating at a speed of 5000 rpm for 60 s and subsequently annealing at 100 ℃ for 10 min in ambient air. After transferring the substrates into nitrogen-filled glove box, the 100 nm thick active layers were deposited by spin-coating from a blended solution of PTB7-Th (10 mg) and $PC_{71}BM$ (15 mg) in chlorobenzene (1 mL) with 3 vol% of DIO under 1500 rpm for 60 s. Finally, the MoO_3 (6 nm) and Ag (100 nm) layers were thermally evaporated through a shadow mask onto the active layer under 2.0×10^{-4} Pa.

Fabrication of electron-only devices: Space charge-limited currents were tested in electron-only devices with the configurations of ITO/Al/ETLs/Al. The mobilities were determined by fitting the dark current to the single-carrier SCLC model at low voltage, which is described as $J=(9/8)\varepsilon_0\varepsilon_r\mu((V^2)/(L^3))$, where J is the current, μ is the electron mobility, ε_0 is the permittivity of free space, ε_r is the relative permittivity of the material, V is the effective voltage, and L is the thickness of the ETL layers. The effective voltage can be obtained by subtracting the built-in voltage (V_{bi}) and the voltage drop (V_s) from the substrate's series resistance from the applied voltage (V_{appl}), $V= V_{appl}-V_{bi}-V_s$.

Fabrication of diodes for conductivity characterization: Photoconductive devices were fabricated with the configuration of ITO/ETLs (100 nm)/Ag (100 nm). The photoconductivity of different layers was recorded under AM 1.5G irradiation with an intensity of 100 mW cm^{-2}. The conductivity was

defined as $\sigma = h/(RA)$, with R as electrical resistance (V/I), A as the active area (6 mm^2), and h as film thickness.

Characterization and measurements: The current density-voltage (J-V) characteristics for the devices were measured in a glovebox using a Keithley 2400 source meter and an Air Mass 1.5 Global solar simulator (Taiwan, Entelich). The irradiation intensity of the light source was calibrated by a standard silicon solar cell with a KG5 filter, modulated a value of 100 mW cm^{-2}. EQE values were tested with a commercial EQE measurement system (Taiwan, Enlitech, QE-R) during illumination with chopped monochromatic light from a xenon lamp. Absorption and transmittance spectra were measured using a UV-vis spectrophotometer (Perkin Elmer Lambda 365). The film thickness was measured using a surface profiler (XP-100). The film surface morphologies were investigated using via atomic force microscopy (Bruker, Innova, Germany) in tapping mode. The surface energy of films was calculated by an surface contact angle meter (Shengding SDC-100, Guangdong). X-ray photoelectron spectroscopy (XPS) measurements were performed by using a Thermo Fisher Scientific PHI Quantera II system with a monochromatic Al Kα source(1,486.6 eV). Ultraviolet photoelectron spectrometer (UPS) measurements of the onset of photoemission for determining the WF were performed using standard procedures with a −10 V bias applied to the sample. Impedance measurements were obtained on the CHI660E electrochemical workstation (CH instruments, Inc.) under a bias of 0.6 V with the amplitude of 50 mV and a dark conditions from high to low frequency (1M to 100 Hz). Equivalent circuit simulations were calculated by a software package ZView 3.1 (Scribner Associate, Inc.).

S2. FT-IR spectra

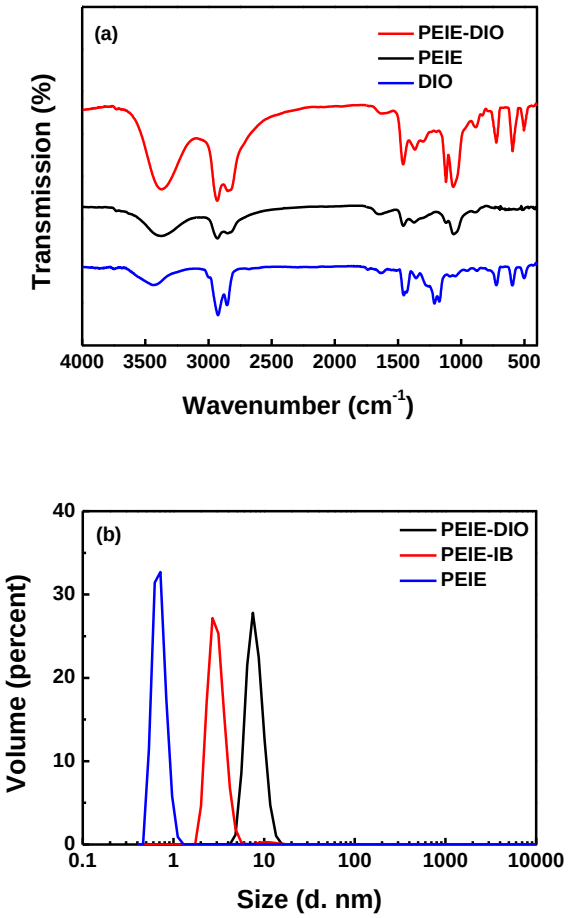

Fig. S1 (a) FT-IR spectra of the PEIE-DIO, PEIE-IB and PEIE films casted on KBr and (b) distribution of particle size for PEIE-DIO, PEIE-IB and PEIE.

S3. photovoltaic performance

At the beginning, the preliminary device optimization was carried out by optimizing weight ratio of PEIE: DIO with a thickness about 10 nm (**Fig. S2**, **Table S1**). The J-V curves are shown in **Fig. S2**. As shown in Table S1, the J_{sc} and PCE values of the devices with PEIE-DIO as the ETL are gradually improved when the weight ratio of PEIE: DIO is changed from 1:1 to 1:4. Subsequently, the photovoltaic performance gradually decreases after the weight ratio is further varied to 1:6 and 1:8. Therefore, all the PSC devices are prepared with the optimized weight ratio of 1:4 in the discussion section unless noted otherwise.

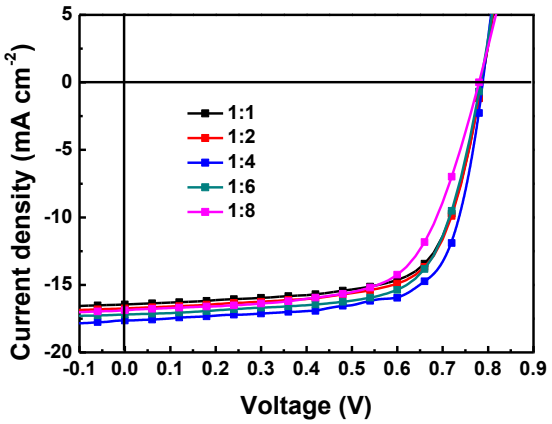

Fig. S2. J-V curves of the PSCs based on PEIE-DIO as the ETL with different weight ratio (PEIE: DIO) under the illumination of AM 1.5G, 100 mW cm^{-2}.

Table S1 Photovoltaic properties of the PSCs based on PEIE-DIO as the ETL with different weight ratio (PEIE: DIO) under the illumination of AM 1.5G, 100 mW cm^{-2}.

PEIE: DIO	J_{SC} (mA cm^{-2})	V_{OC}(V)	FF	PCE (%)	best PCE (%)
1: 1	16.28±0.17	0.78±0.01	0.68±0.01	8.63±0.34	8.97
1: 2	16.61±0.14	0.78±0.01	0.68±0.01	8.81±0.32	9.13
1: 4	17.54±0.14	0.79±0.00	0.71±0.01	9.84±0.22	10.06
1: 6	17.01±0.19	0.77±0.01	0.68±0.01	8.91±0.35	9.26
1: 8	16.66±0.22	0.77±0.01	0.63±0.02	8.08±0.48	8.56

To evaluate the effects of the thickness of ETLs on photovoltaic performances, the preliminary device optimization was carried out. The J-V curves are shown in **Fig. S3**, and their corresponding parameters are summarized in **Table S2**. As shown in **Table S2**, the J_{SC}, FF and PCE values of the devices with PEIE as the ETL are rapidly reduced with the increase of the thickness. Relatively, the J_{SC}, FF and PCE values of the devices with PEIE-DIO as the ETL are only slightly reduced with the increase of the thickness. Simultaneously, no S-shaped J-V curves are observed in the devices with PEIE-DIO as the ETL under different thicknesses (9-50 nm), indicating no evident enhancement of series resistance (R_s) and reduction of shunt resistance (R_{sh}) in the devices (**Fig. S3b**).

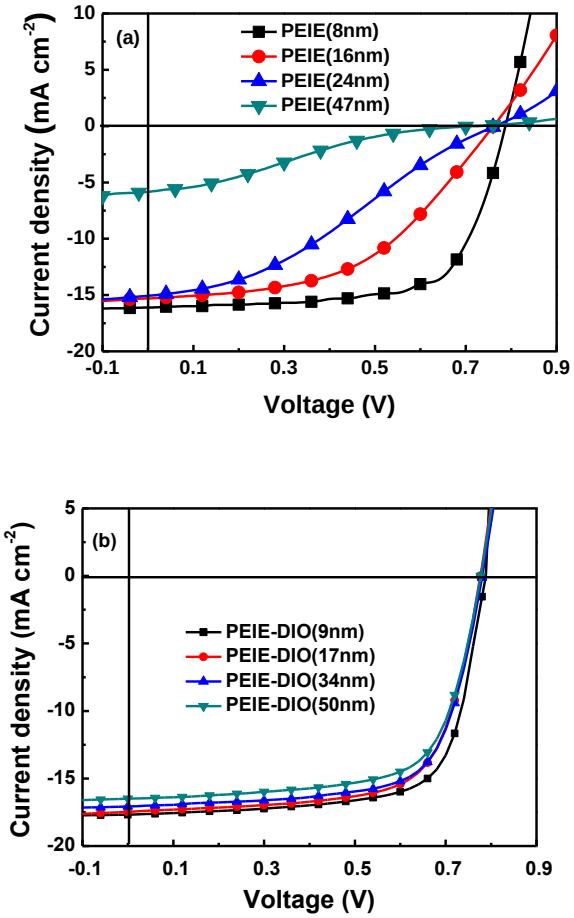

Fig. S3 J-V curves of the PSCs based on PEIE (a) and PEIE-DIO (b) as the ETLs with various thicknesses under the illumination of AM 1.5G, 100 mW cm^{-2}.

Table S2. Photovoltaic properties of the PSCs based on PEIE and PEIE-DIO as the ETLs with various thicknesses under the illumination of AM 1.5G, 100 mW cm^{-2}.

ETLs	Thickness	J_{SC} (mA/cm^2)	V_{OC} (V)	FF	PCE(%)	best PCE(%)
PEIE	8 nm	15.95±0.16	0.78±0.01	0.67±0.01	8.42±0.23	8.65
	16 nm	15.14±0.16	0.75±0.01	0.47±0.02	5.41±0.39	5.70
	24 nm	14.84±0.23	0.75±0.01	0.31±0.02	3.49±0.29	3.78
	47 nm	5.36±0.47	0.70±0.02	0.19±0.04	0.71±0.26	0.97
PEIE-DIO	9 nm	17.54±0.14	0.79±0.00	0.71±0.01	9.84±0.22	10.06
	17 nm	17.44±0.03	0.77±0.01	0.68±0.01	9.25±0.15	9.40
	34 nm	17.05±0.02	0.77±0.01	0.68±0.01	9.02±0.17	9.19
	50 nm	16.29±0.21	0.77±0.01	0.67±0.02	8.56±0.32	8.88

S4. Contact angle measurements

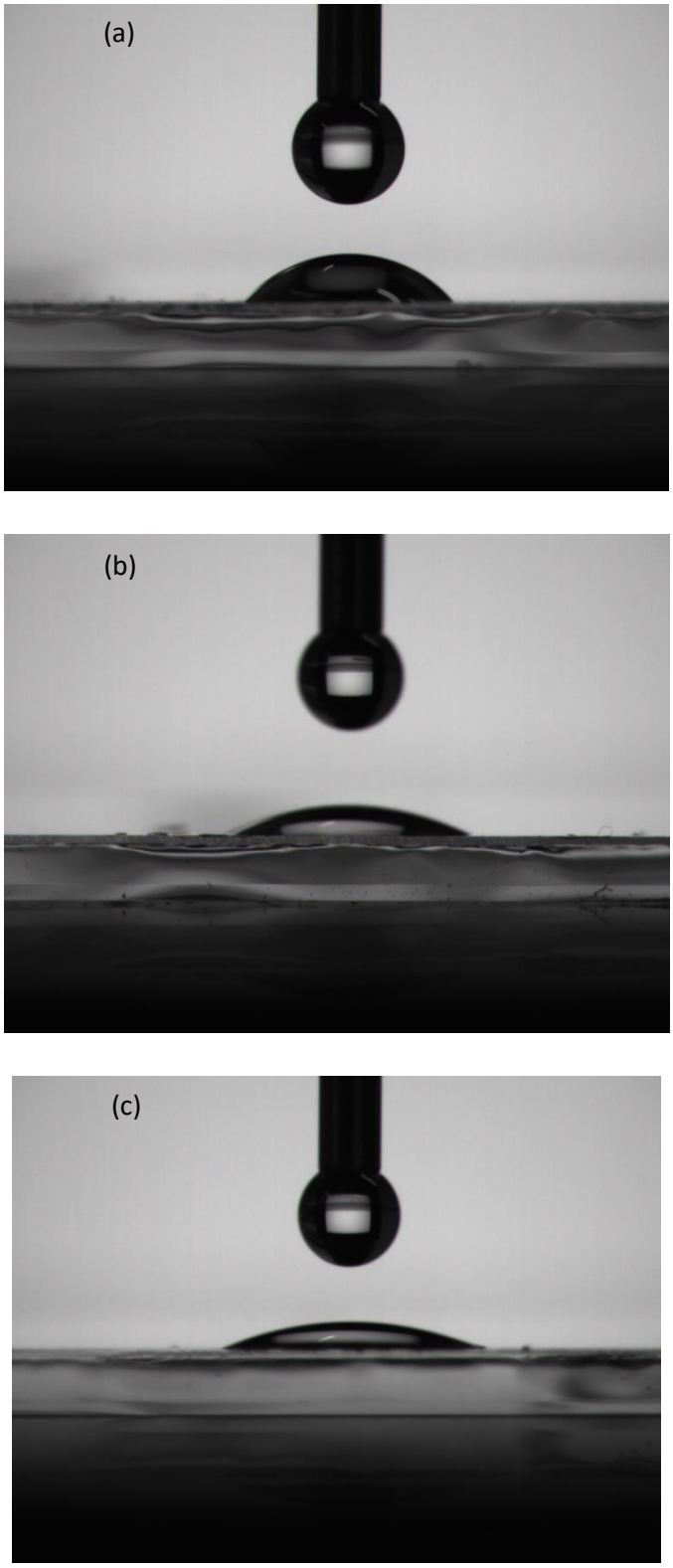

Fig. S4 Contact angle measurements of (a) PEIE-DIO, (b) PEIE-IB and (c) PEIE on ITO glass (deionized water).

S5. Morphology

The film morphology of PEIE-DIO, PEIE-IB and PEIE on ITO glass substrate was studied using atomic force microscopy (AFM). As shown in **Fig. S5**, PEIE-IB (**Fig. S5b**) and PEIE (**Fig. S5c**) films possess similar phase images. Compared with PEIE-IB and PEIE films, PEIE-DIO film shows obviously different phase image (**Fig. S5a**). As shown in **Fig. S6 a-c**, three kinds of ETL films possess smooth and homogenous surface morphology with similar surface root mean square roughness values of 0.98 nm for PEIE-DIO, 1.00 nm for PEIE-IB and 1.06 nm for PEIE. According to **Fig. S5 d-f** and **Fig. S6 d-f**, the smallest domain size (**Fig. S5d**) in the active layer on PEIE-DIO film proves better phase separation of donor and acceptor in active layers.

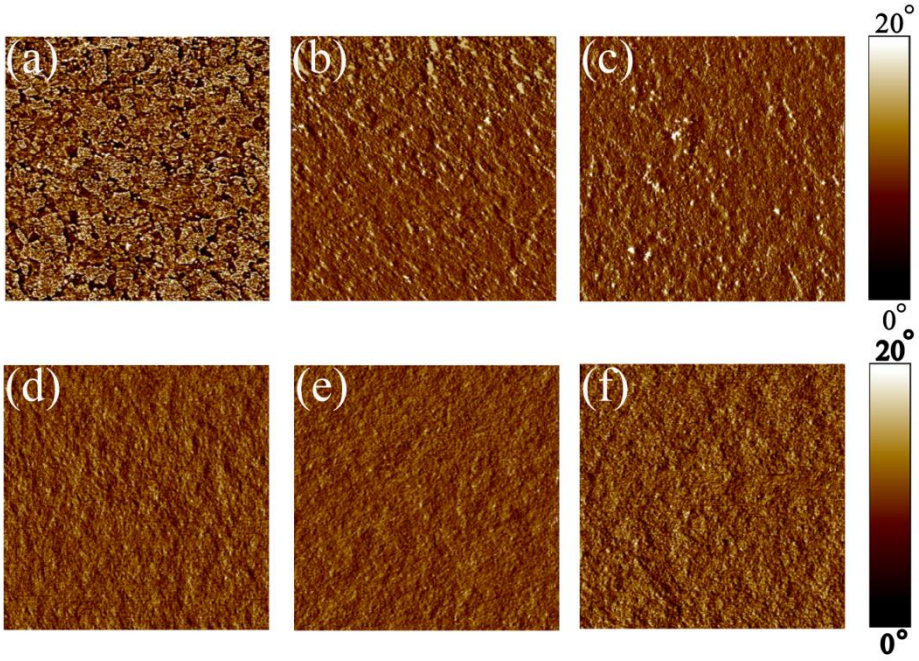

Fig. S5 AFM phase images (3 μm×3 μm) of (a) PEIE-DIO/ITO, (b) PEIE-IB/ITO (c) PEIE/ITO, (d) PTB7-Th: $PC_{71}BM$/PEIE-DIO/ITO, (e) PTB7-Th: $PC_{71}BM$/PEIE-IB/ITO, and (f) PTB7-Th: $PC_{71}BM$/PEIE/ITO.

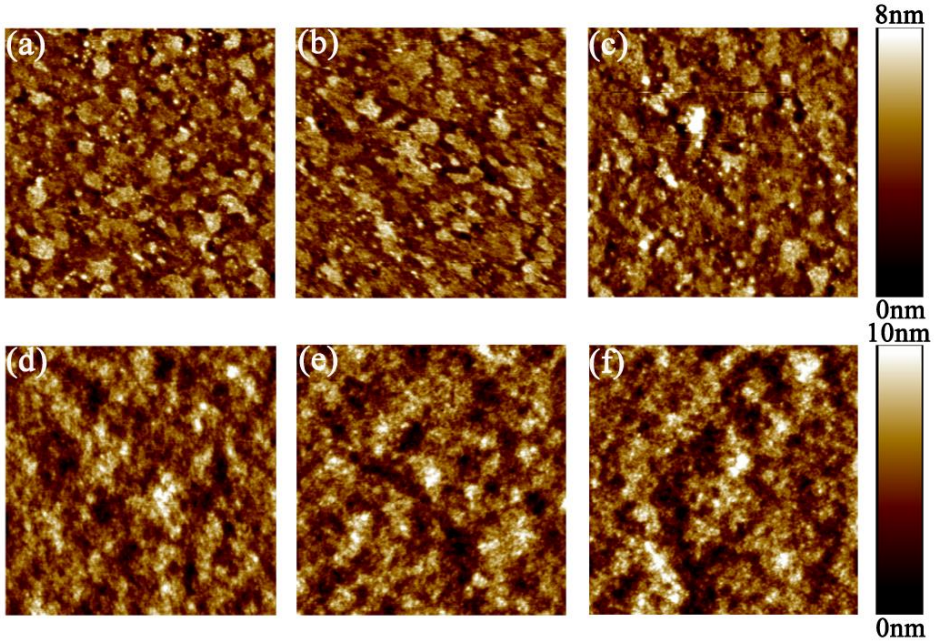

Fig. S6 AFM height images (3 μm×3 μm) of (a) PEIE-DIO/ITO, (b) PEIE-IB/ITO (c) PEIE/ITO, (d) PTB7-Th: $PC_{71}BM$/PEIE-DIO/ITO, (e) PTB7-Th: $PC_{71}BM$/PEIE-IB/ITO, and (f) PTB7-Th: $PC_{71}BM$/PEIE/ITO.

S6. Electrical impedance spectra

To better understand the electron extraction capability, the charge-transfer resistances (R_{CT}) of the devices with the configuration of ITO/ETLs /PTB7-Th: $PC_{71}BM/MoO_3$/Ag were measured by electrochemistry impedance spectra (EIS). **Fig. S7** shows Nyquist plots for the devices with PEIE, PEIE-IB, and PEIE-DIO as the ETLs. The devices with PEIE-DIO (9 nm), PEIE-IB (8 nm), and PEIE (8 nm) as the ETLs exhibit the R_{CT} values of 25.8, 43.2 and 92.4 Ω cm^2, respectively. Therefore, the PEIE-DIO-based device possesses the best effective charge transfer on the interface of ITO/ETLs and ETLs/photoactive layer.

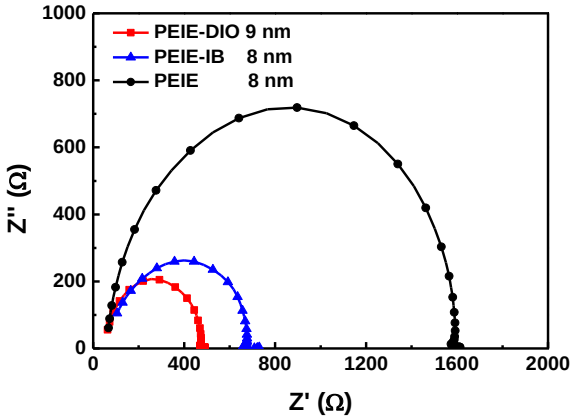

Fig. S7. Electrical impedance spectra of the PSC devices based on the different ETLs.

S7. Stability

To investigate the effects of the ELTs on device stability, the devices with different ETLs were kept for a period of time under ambient conditions (30% relative humidity) in the dark, and the PCE-time curves are shown in **Fig. S8**. After kept for 250 hours, the device based on PEIE–DIO retains over 83% PCE value, but the PEIE-based device only retains about 76% PCE value. As shown in **Fig. S4**, PEIE-DIO, PEIE-IB and PEIE -covered ITO exhibit the contact angles of 55.2°, 28.8° and 29.0°, respectively. Therefore, the corresponding surface energy of PEIE-DIO, PEIE-IB and PEIE -modified ITO are 44.9 mN m^{-1}, 51.4 mN m^{-1} and 51.9 mN m^{-1}. Compared with PEIE, PEIE-IB possesses similar surface energy, which indicates that quaternarization does not change hydrophilism of PEIE. However, PEIE-DIO possesses the largest surface contact angle (55.2°) and smaller surface energy (44.9 mN m^{-1}), which indicates that the cross-linked structure of PEIE-DIO depresses its hydrophilicity property since quaternarization does not change hydrophilicity property of PEIE. Therefore, PEIE–DIO possesses lower hydrophilism than PEIE, so the PSC device based on PEIE–DIO shows better device stability in ambient conditions (**Fig. S8**).

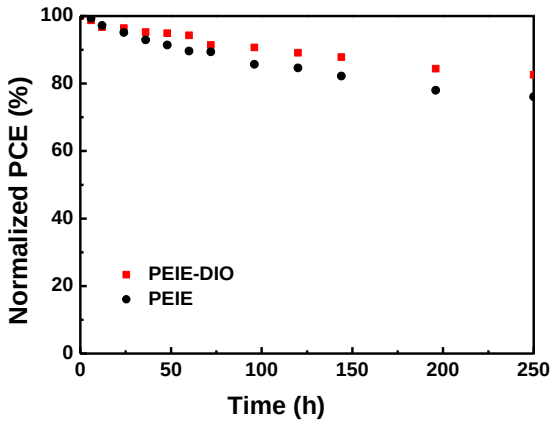

Fig. S8 Device stability in ambient condition.